The Biorhythm of Human Skeletal Growth

Patrick Mahoney[1], Justyna J. Miszkiewicz[2], Simon Chapple[1], Mona Le Luyer[1,3], Stephen H. Schlecht[4], Tahlia J. Stewart[2], Richard A. Griffiths[5], Chris Deter[1], Debbie Guatelli-Steinberg[6]

[1]Human Osteology Lab, Skeletal Biology Research Centre, School of Anthropology and Conservation, University of Kent, Canterbury, UK.

[2]Skeletal Biology and Forensic Anthropology Research Group, School of Archaeology and Anthropology, Australian National University, Canberra, Australia.

[3]De la Prehistoire à l'Actuel Culture Environment et Anthropologie (PACEA), University of Bordeaux, Aquitaine, France.

[4]Department of Orthopaedic Surgery, University of Michigan, Ann Arbor, MI, USA.

[5]Durrell Institute of Conservation and Ecology, School of Anthropology and Conservation, University of Kent.

[6]Department of Anthropology, The Ohio State University, Columbus, OH, USA .

Correspondence

Patrick Mahoney. Human Osteology Lab, Skeletal Biology Research Centre,
School of Anthropology and Conservation,
University of Kent, Canterbury. UK. CT2 7NR.
E: p.mahoney@kent.ac.uk
T: +44 1227 764 7927

Text pages = 19 + bibliography = 6
Figures = 6
Tables = 2
Supporting information = 1

Abbreviated title

The biorhythm of human skeletal growth

KEYWORDS

Retzius line periodicity. Enamel thickness. Daily enamel secretion rates. Osteocyte lacunar density. Stature.

Abstract

Evidence of a periodic biorhythm is retained in tooth enamel in the form of Retzius lines. The periodicity of Retzius lines (RP) correlates with body mass and the scheduling of life history events when compared between some mammalian species. The correlation has led to the development of the inter-specific Havers-Halberg Oscillation (HHO) hypothesis, which holds great potential for studying aspects of a fossil species biology from teeth. Yet, our understanding of if, or how the HHO relates to human skeletal growth is limited. The goal here is to explore associations between the biorhythm and two hard tissues that form at different times during human ontogeny, within the context of the HHO. First, we investigate the relationship of RP to permanent molar enamel thickness and the underlying daily rate that ameloblasts secrete enamel during childhood. Following this, we develop preliminary research conducted on small samples of adult human bone by testing associations between RP, adult femoral length (as a proxy for attained adult stature), and cortical osteocyte lacunae density (as a proxy for the rate of osteocyte proliferation). Results reveal RP is positively correlated with enamel thickness, negatively correlated with femoral length, but weakly associated with the rate of enamel secretion and osteocyte proliferation. These new data imply that a slower biorhythm predicts thicker enamel for children but shorter stature for adults. Our results develop the intra-specific HHO hypothesis suggesting that there is a common underlying systemic biorhythm that has a role in the final products of human enamel and bone growth.

Introduction

Biorhythms are cyclic changes in an organism's growth, development, or functioning that are driven by an internal biological 'clock' and synchronized through environmental cues (Hastings, 1998). They have been linked to variations in human body temperature, metabolism, testosterone production, ovulation, and rate of tooth eruption (Reinberg et al., 1965; Little and Rimmel, 1971; Sothern, 1974; Lee and Profitt, 1995; Garde et al., 2000). Human tooth enamel retains evidence of periodic fluctuations that occur as enamel forming cells (secretory ameloblasts) deposit mineralising protein matrix (Retzius, 1837; Asper, 1916). One of these fluctuations manifests as cross striations, which are incremental enamel markings that correspond with a circadian rhythm (Schour and Poncher, 1937; Boyde, 1979, 1989; Risnes, 1986; Bromage 1991; Antoine et al., 2009; Lacruz et al., 2012; Zheng et al., 2013). Another longer-period infradian rhythm leads to enamel Retzius lines (e.g., Dean, 1987; Risnes, 1990; Beynon, 1992). Retzius lines mark 'layers' of forming enamel that are usually separated by six to 12 days of growth in human permanent teeth (**Fig. 1**), depending upon the individual (Schwartz et al., 2001; Reid and Dean, 2006; Reid and Ferrell, 2006; Mahoney, 2008). The Havers Halberg Oscillation (HHO) hypothesis proposes that Retzius line periodicity (RP), the number of days between adjacent Retzius lines, is a manifestation of a central infradian biorhythm that regulates the rate of bone cell proliferation and adult body mass via metabolism, with links to life history traits, when compared between some mammalian species (Bromage et al., 2009, 2012). Much less is known about the potential role of this oscillation for human skeletal growth. Here, we extend our previous intra-specific research into the HHO in which we established associations between human deciduous enamel growth and RP (Mahoney et al., 2016; 2017). We construct and test predictions about the relationship of RP to human permanent enamel thickness and the underlying daily rate that enamel forms during the childhood years. We develop preliminary research conducted on small samples of adult human bone (Bromage et al., 2016a), by assessing the relationship of

adult femoral length and the underlying density of bone maintenance cells (osteocytes) to RP. Our goal is to explore the periodicity of the biorhythm against two hard tissues that form at different but overlapping times during human ontogeny, within the context of the HHO.

Enamel biorhythms of mammals and the Havers-Halberg Oscillation hypothesis

Research into relationships between the periodicity of Retzius lines and somatic growth commenced in the 1990's with those that suspected RP might relate to mammalian body size (Dean, 1995; Dean and Scandrett 1996). Soon after, studies established a significant inter-specific positive correlation between RP and average body mass in a selection of extant and fossil mammals (Smith et al., 2003; Smith, 2008; Bromage et al., 2009). Not all primate species followed this pattern (Hogg et al., 2015), and a lower rather than a higher RP related to a larger estimated body mass for three fossil species (Schwartz et al., 2002, 2005; Le Cabec et al., 2017). Further work reported inter-specific associations between the periodicity of the biorhythm and the scheduling of life history traits for some primate species (Bromage et al., 2012). The inter-specific HHO hypothesis developed out of these studies, and earlier research on mammals (Mullender et al., 1996; Bromage et al., 2009, 2012).

The hypothesised biological 'clock' that regulates Retzius lines is unknown, but given that RP subdivides into multiples' of daily intervals, the suprachiasmatic nucleus of the hypothalamus (SCN) has been identified as one likely contender (Bromage et al., 2012). The SCN is a source of circadian rhythmic activity in mammals (Richter, 1965; Ralph et al., 1990; Sujino et al., 2003) and has a role in regulating metabolism via the pituitary gland (Weaver, 1998; Kalsbeek et al., 2011; Coomans et al., 2013). The HHO hypothesis drew upon this biological pathway proposing that Retzius lines were a manifestation of a longer-period oscillation stemming from the hypothalamus that employed SCN 'machinery' in its pathway to stimulate pituitary secretions that linked to metabolism, body mass, and primate life history traits (Bromage et al., 2012). Experimental research on domestic pig links aspects of

metabolism to RP (Bromage et al., 2016b). Further support for an inter-specific HHO is provided by some mammalian species with slower metabolisms, and a larger body size combined with a higher mean RP, relative to those with smaller body size (Bromage et al. 2009).

Enamel biorhythms of humans and the Havers-Halberg Oscillation hypothesis

The idea that human enamel growth might be controlled by an underlying biological 'clock' is not a new one, as the presence of daily cross-striations along enamel prisms implies that secretory ameloblasts may be under circadian control via clock genes (maintainers of circadian rhythms) during amelogenisis (Schour and Poncher, 1937; Bromage, 1991; Antoine et al., 2009; Lacruz et al., 2012; Zheng et al., 2013). However, much less is known about the potential role of the longer-period HHO for human enamel growth. Recently we reported links between RP, the width of enamel 'layers' between adjacent Retzius lines, and two dimensional (2D) average and relative enamel thickness of human deciduous maxillary second molar crowns (dm^2) (Mahoney et al., 2016, 2017). We also identified an association between RP and dm^2 paracone cusp formation time (Mahoney et al., 2016). The relationship of RP to daily enamel secretion rates (DSRs) was however less clear. When RP and DSRs were calculated for dm^2 in one homologous dental location and compared between individuals there was a weaker association between these variables (Mahoney et al., 2017). Prior to our research, enamel growth had not been considered within the context of the HHO hypothesis. Based upon our data, we proposed that if RP is evidence of the HHO, an underlying biorhythm that affects physiological systems (Bromage et al., 2009, 2012), then its influence extends to enamel thickness and formation time of deciduous molar enamel, but was less clearly associated with deciduous DSRs (Mahoney et al., 2017). Up until now, no study has determined if there is a relationship between RP and human permanent molar enamel thickness, or DSRs calculated for this tooth type.

Research on four adult humans hints at a negative correlation between adult stature and RP (Bromage et al., 2016a). This shift away from the positive correlation reported in inter-specific research on mammalian species (see above) is to be expected within the context of the HHO. Inter-specifically, mammals with larger bodies tend to have an extended growth period with slower rates of metabolism and associated cell proliferation, which is reflected by a higher mean RP (and thus slower oscillation of the biorhythm) relative to smaller bodied species (Mullender et al., 1996; Bromage et al., 2009). Within humans, the growth period is constrained between birth and adulthood, so greater stature is achieved by 'speeding up' the biorhythm (reducing the periodicity), and thus increasing skeletal metabolism or the rate of cell proliferation (Bromage et al., 2016a). Thus, our current understanding of the HHO is that inter-specific scaling trends between RP and body size may be associated with alterations in the *duration* of development, whereas within humans, RP may relate to adult stature through variation in growth *rates* (Bromage et al., 2009).

Preliminary support for the HHO hypothesis within humans is provided by a study of bone osteocyte lacunar density (Ot.Dn) (Bromage et al., 2016a). Osteocytes are former osteoblasts that become trapped as they finish producing bone matrix (e.g., Palumbo et al., 1990). These cells have a complex functionality, that includes sensing mechanical (shear or strain) forces applied to bone, which activates remodeling via the linked action of osteoblasts and osteoclasts (e.g, Frost, 1987; Robling and Turner, 2002; Mullender et al., 2007; Bonewald, 2007; Tatsumi et al., 2007; Noble, 2008); detecting and initiating micro-damage repair (e.g., Verborgt et al., 2000; Herman et al., 2010); and in mineral homeostasis (e.g., Cullinane, 2002; Teti and Zallone, 2009; Nakashima et al., 2011). The Ot.Dn of healthy bone can also vary when compared to pathological bone (e.g., Mullender et al; 2005; van Hove et al, 2009). In addition to these potential influences, Ot.Dn can correspond with body size, whereby Ot.Dn of the mid-shaft femur from 12 adult humans scaled positively with final attained adult stature (Bromage et al., 2016a). This scaling relationship suggests that the rate

of osteocyte proliferation is greater in taller adult individuals, which is consistent with the hypothesised effect of the HHO on human body size.

Research questions and predictions

The background research provides a foundation from which to formulate four research questions, and from these, predictions, that will be tested by calculating RP from thin sections of teeth and comparing these values to measures of human skeletal growth. The research questions are as follows:

Do daily enamel secretion rates correlate with RP in permanent molars?

We have previously shown RP does not exert a consistent influence on the daily rate that ameloblasts secrete structural matrix proteins as they increase the length of hydroxyapatite crystallites in deciduous enamel (Mahoney et al., 2017). Instead, it seems more likely from links we have reported, and by others, that the intra-specific HHO is related to the end state of enamel growth (i.e., final enamel thickness) through formation time. These links commence as ameloblasts secrete matrix for an additional number of days between adjacent Retzius lines, leading to thicker 'enamel layers' with higher RP's (Mahoney et al., 2017). Layers become thicker because ameloblasts do not greatly alter their DSRs in outer lateral enamel regions as RP increases, when compared between human molars from different individuals. Thicker layers accumulate leading to greater average enamel thickness (AET) of dm^2 crowns with higher RP's, relative to molars with lower RP's (Mahoney et al. 2016). Thicker crown enamel takes a longer period of time to form, for deciduous molars (Mahoney 2011), and permanent teeth (Dean et al., 2001). Formation time is correlated with RP, for deciduous molar paracone cusps (Mahoney et al., 2016) and for permanent mandibular canine lateral enamel (Reid and Ferrell, 2006). Thus, unlike the HHO intra-specific prediction for body mass, where RP links to final attained adult stature through variation in growth rates (Bromage et al., 2009), we suggest that RP is not strongly related to final enamel thickness

via daily enamel secretion rates (and is thus more likely to be related to enamel formation time). Thus, we predict a weak association between RP and DSRs of permanent molars. To examine the relationship between the circadian and the infradian rhythm in permanent enamel, we separated out *n*=15 M1's from our sample, and calculated and compared RPs and DSRs in one homologous location in outer lateral enamel of each crown.

Does permanent molar enamel thickness correlate with RP?

Two dimensional measurements of AET from human dm^2 correlated positively with RP (Mahoney et al., 2016). Assuming that RP is evidence of a biorhythm that affects multiple physiological systems, including enamel growth, then we predict that its influence will extend to permanent molar enamel thickness. To test this prediction we calculate 2D AET and enamel area (EA) for human permanent first (M1) and second molars (M2) from thin sections, and compare these values to RP's of the same teeth. Based upon findings for deciduous molars, RP of permanent molars should scale positively with our measures of enamel thickness.

Is adult femoral length correlated with RP?

The intra-specific HHO predicts that greater adult height is achieved through a biorhythm that is accelerated (Bromage et al. 2016a), with a shorter periodicity. To assess RP against stature, we selected a sample of younger adult males with shorter femora, and compared these to younger adult males with longer femora. We calculated RP for each male and compared this value to his stature (reconstructed from femoral length). The femur has been used within regression equations for the past fifty years to reconstruct stature (e.g., Trotter, 1970; and see methods). We also compare RP to femoral length.

Is adult femoral length correlated with cortical bone osteocyte lacunae density?

The intra-specific HHO predicts that taller humans (with longer femora) grow more rapidly with a faster rate of osteocyte proliferation, relative to shorter individuals. Data for 12 individuals indicate these faster rates are then maintained as adults (Bromage et al., 2016a). As Ot.Dn can sometimes vary with age (e.g., Mullender et al., 1996) we subdivided our entire adult male sample into age groups and explored associations between Ot.Dn and stature, within each group. We also assess Ot.Dn against adult femoral length, and against RP.

Materials and Methods

Our samples are human skeletons from one cemetery in Canterbury, England, that dates to the early 16th century AD (Hicks and Hicks, 2001). Historical texts state that burials were from a single lower socio-economic group that lived and worked in Canterbury and represented non-catastrophic mortality (Somner 1703; Duncombe 1785; Brent 1879). We have previously shown that the periodicity of the biorhythm can change in response to non-specific pathology (Mahoney, et al., 2017). We limited this type of variation in our data by only selecting skeletons and teeth without skeletal or radiographic signs of pathology, drawing upon an extensive collection of accompanying radiographs that were produced at Kent and Canterbury Hospital (Radiology Department) for any skeleton with suspected trauma or pathology. Age-at-death is reconstructed for all skeletons; sex is reconstructed for adults (see Methods). These collections are curated in the Skeletal Biology Research Centre, University of Kent, UK. All sectioning adhered to the British Association of Biological Anthropology and Osteoarchaeology code of practice (2014). No permits were required for this study as these are archaeological samples from before the 19th Century AD.

Samples and the chronology of skeletal growth

We selected three samples. Throughout, RP is calculated for lateral enamel of permanent M1 and M2. Lateral enamel of these tooth types forms between approximately 1.5 to 5.7 years of age (Reid and Dean, 2006). Sample sizes varied depending upon the variables examined and are given in the corresponding tables. One tooth (either M1 or M2) represents one individual. Raw data is available in Supporting Information.

a) The first sample was juveniles (n=40). We assessed RP against daily enamel secretion rates, and against enamel thickness of the same molars. We chose juveniles (<8yrs of age for M1's; <13yrs for M2's) because enamel is often worn in adults, and this would have affected our measurements of 2D AET and EA. Daily enamel secretion rates of M1 and M2 are a measure of the rate that ameloblasts previously deposited matrix during the secretory phase of enamel growth in the childhood years. Average enamel thickness and EA of M1 and M2 are a measure of the end state of the secretory stage of enamel growth that is attained in childhood.

b) The second sample was young adult males, aged between 18 to 34yrs (n=27). We assessed RP of their M1 or M2 (representing their childhood years), against their femoral cortical bone osteocyte lacunar density, and final attained adult stature. Osteocyte lacunar density in adult cortical bone likely represents a combination of lamellae deposited during later ontogeny and in adulthood. Final attained adult stature is the end state of linear growth of long bones via endochondral ossification over the course of postnatal development from birth to adulthood. In this study, we measure adult femoral length as a proxy for attained adult stature. The slight occlusal wear of some molars did not affect our calculation of RP in lateral enamel, which is located cervical to wear on the occlusal surface. We did not include older adults because of their greater enamel wear.

c) The third sample was adult males, subdivided into two age groups (younger males 18-34yrs, *n*=28; older males 35-50yrs, *n*=94). We assessed femoral cortical Ot.Dn against their estimated stature, and femoral length.

Sample preparation for histology

We used standard histological techniques (Bancroft and Gamble, 2008; Mahoney, 2008; Miszkiewicz, 2016). Each tooth was embedded in polyester resin to reduce the risk of splintering while sectioning. Using a diamond-wafering blade (Buehler® IsoMet 4000 precision saw), buccal-lingual sections captured the paracone and protocone of maxillary molars and the protoconid and metaconid of mandibular permanent molars. Each section was mounted on a microscope slide, lapped using a graded series of grinding pads (Buehler® Eco-Met 300) to reveal incremental lines, polished with a 0.3μm aluminum oxide powder (Buehler® Micro-Polish II), placed in an ultrasonic bath to remove surface debris, dehydrated through a series of alcohol baths, cleared (Histoclear®), and mounted with a coverslip using a xylene-based mounting medium (DPX®).

Dry, un-decalcified bone measuring 1cm in depth was removed from the posterior femoral mid-shaft cortex using a drill (Dremel Rotary®) with a circular metal blade (**Fig. 2**). Only the posterior portion of the femoral diaphysis was used in order to keep the overall integrity of the femur preserved for future research purposes. The bone was embedded in epoxy resin, reduced in thickness (Buehler® IsoMet 4000 precision saw), ground, polished, and cover-slipped following the same procedures used to embed and prepare the teeth. Thin sections measured approximately 100μm in depth.

Retzius line periodicity

Using a high-resolution microscope (Olympus® BX51), each section was examined at magnification (10-60x). Images were captured with a microscope digital camera (Olympus® DP25) and analyzed in CELL® Live Biology imaging software. We counted the number of cross-striations along a prism between several adjacent Retzius lines in outer lateral enamel of M1 and M2 to determine the number of days between two adjacent Retzius lines. For twelve thin sections, cross-striations were not clearly visible and continuous along prisms between adjacent Retzius lines. For these twelve sections, we divided the distance between several adjacent Retzius lines by local mean daily secretion rates (e.g., Schwartz et al., 2001; Mahoney et al., 2007; Lacruz et al., 2008). We did not include these sections in the analysis of RP and secretion rates. Retzius periodicity was recorded by SC and PM. After they had finished recording all slides they conducted an inter-observer error test. The test revealed one difference in RP calculations between the two observers. This slide was removed from the study.

Enamel thickness

The 2D AET in mm was calculated by dividing the area of the enamel cap (EA) by the length of the dentin-enamel junction (DEJ), which provides the average straight-line distance between the DEJ and outer enamel surface (Martin, 1983, 1985). EA is given in mm^2.

Enamel daily secretion rates

Secretion rates in μm per day were calculated for outer lateral enamel in the same region that we recorded RP (ie., avoiding inner and mid enamel regions as DSRs can vary from one region to the next within a crown: Lacruz and Bromage 2006). Rates were measured along the long axis of an enamel prism. A distance corresponding to five days of enamel secretion was measured, and then divided by five to yield a mean daily rate. The procedure was repeated a minimum of six times in each region, which allowed a grand mean value and

standard deviation (SD) to be calculated. The grand mean value was compared to RP calculated in the same enamel region.

Osteocyte lacunae density

We use Ot.Dn as a proxy for the rate of (past) femoral cortical bone cell proliferation. Osteocyte lacunae density data were collected as part of a PhD project (Miszkiewicz, 2014). We selected femoral Ot.Dn, rather than osteon population density, so that we could directly test prior research (see above). Osteocyte lacunae density is significantly correlated with osteon population density in this skeletal sample (Miszkiewicz, 2016). Exploring associations between Ot.Dn and age, or at the initiation of remodeling (e.g., Metz et al., 2003), were not aims of this study.

Using a high-resolution microscope (Olympus® BX51, and Olympus DP25 microscope camera) osteocyte lacunae were counted within secondary osteonal bone and interstitial bone. Ot.Dn were counted from a maximum of six main regions of interest (ROI; mag =10X, 2.44 mm^2) positioned adjacent to the periosteum, and sub-divided into smaller ROIs (mag =40X, 0.13 mm^2) (**Fig. 2**). See Miszkiewicz (2016) for a detailed methodology of ROI's. Using CELL® Live Biology Imaging software, all visible osteocyte lacunae (including cavities which appeared "empty" or transparent) were counted using a "touch count" tool (identical in premise to the "point count technique" recommended by Parfitt, 1983). Densities were calculated by dividing the total number of osteocyte lacunae by the area of bone examined (in mm^2). We acknowledge that automated methods of osteocyte lacunae detection are available, and ideally a whole long bone cross-section should be examined (e.g. Hunter and Agnew, 2016). However, those techniques are better suited to fresh or "recent" bone with excellent microstructural preservation. Given the archaeological background (localised diagenetic alteration of micro-anatomy) of our samples, there needed to be flexibility in our ROI selection procedures. This is because the ROI would sometimes have to be moved

fractionally to avoid an area of diagenesis or one that was affected by taphonomy. Clear differences in osteocyte lacunar densities were observed across the sample (see **Fig. 2**).

Stature estimation and femoral length

Femoral length data were previously included in robusticity index calculations as part of another project (Miszkiewicz and Mahoney, 2016), but correlations between Ot.Dn and stature/femur length are examined here for the first time. The maximum length of each femur was measured by placing it flat on an osteometric board, in its anatomical position, with the posterior femoral aspect facing down. Femoral length was measured from the most superior surface of the femoral head to the most distal surface of the medial condyle (Buikstra and Ubelaker, 1994). Standard, and most commonly used formulae for reconstructing stature in skeletal remains were used (Trotter, 1970; White et al., 2011). These were specific to sex and appropriate for individuals of European descent. Male stature was estimated using the regression equation: 2.38 x femur maximum length in cm + 61.41 (+/- 3.27) (Trotter, 1970; White et al., 2011).

Sex determination and age-at-death

Sex determination was carried out using multiple standard methods to increase the accuracy of the determination. We relied upon standard morphological characteristics of the pelvis and cranium. The pelvic methods were based upon 25 morphological characteristics of the human pelvis taken from Schwartz (1995), Ferembach et al., (1980), Krogman and Iscan (1986) and Phenice (1969). Cranial features included the mastoid process, supraorbital margin, mental eminence, and nuchal crest (Buikstra and Ubelaker, 1994). When determinations from cranial and pelvic features conflicted, priority was given to the pelvic criteria (White et al., 2011). In the analyses, 'probable males' were classified as male.

Age was estimated from age-specific morphology of the pubic symphysis, and the auricular surface of the pelvis (e.g., Meindl et al., 1985; Lovejoy et al., 1985). Two age categories were constructed: younger adult males, 18-34 years; older adult males 35-50 years.

Analyses

Data were analyzed in IBM SPSS® 22 (2014). Each variable was log-transformed. A one sample Kolmogorov-Smirnov test indicated that the distribution of the data for each variable was normal. Data from right and left femora (one femur was selected from each individual, and either the right or left depending upon preservation) were pooled. We analyze the data using linear regression statistics. In Tables 1-2 we present the r^2 value (coefficient of determination) which measures the proportion of explained variation, and we also show the r value (correlation coefficient) which measures the strength and direction of the relationship between variables. The residual, presented as a percentage in the Tables, is the error not explained by the regression equation.

Results

Retzius line periodicity, enamel thickness and secretion rates

Regression statistics are in Table 1. Corresponding data for the sample of juveniles is available in Supporting Information Table S1. When data for all tooth types are combined, the enamel areas and AET of permanent molar crowns were significantly and positively related with RP, increasing from minimum values that were associated with an RP of 6 days to maximum values that were associated with RP's of 10 and 11 days respectively (**Fig 3a. Fig 4a**). When subdivided into either M1's or M2's and re-analyzed, RP was significantly related to EA and AET (Table 1). When further subdivided into upper or lower molars, RP was significantly related to EA (**Fig 4b-d**). AET was also significantly related to RP for each upper and lower molar type, except lower M2 where this relationship approached significance (r^2=0.287; p=0.072).

When 15 permanent first molars were separated from the sample, and RPs and DSRs were measured and compared between the molars in one homologous location in outer lateral enamel of each crown, there was no consistent or significant association with the periodicity of Retzius lines.

Retzius line periodicity, femoral length and osteocyte lacunae density

Regression statistics are in Table 2. The corresponding data sets for younger and older male adults are available in Supporting Information Tables S2 and Table S3. Estimated stature (and femoral length) was significantly and negatively related with RP (**Fig. 3b**). The density of osteocyte lacunae did not relate significantly with RP (Table 2). Osteocyte lacunae density was not significantly related to femoral length or stature for younger males (Table 2). There was a weak relationship between these latter variables that approached significance in older males though the residual was high (r^2=0.030; p=0.089).

Discussion

This study builds upon our previous work that examined relationships of RP to human deciduous molar enamel growth, and extends preliminary research into associations between RP and human adult femoral cortical bone growth (Bromage et al., 2016a; Mahoney et al., 2016, 2017). We examined the relationship of permanent molar daily enamel secretion rates to RP, and of osteocyte proliferation to RP. We find limited evidence for either of these relationships, but did find stronger evidence of linkages between RP, permanent molar enamel thickness, and stature.

Retzius line periodicity, enamel thickness and secretion rates

Our data support the prediction that the periodicity of the biorhythm is associated with enamel thickness when considered within a smaller intra-specific scale, within humans. However, as with deciduous molars (Mahoney, et al., 2016), RP was more weakly associated with DSRs, when compared between permanent molars from different individuals. Therefore, even though RP is calculated by a count of cross striations, variation in the biorhythm is not always associated with the *amount* of matrix deposited by ameloblasts in 24 hour periods (**Fig. 5**). Instead, it seems likely that RP can link to the final enamel thickness of a human crown through formation time. RP is related to the time taken to form part of a deciduous and permanent tooth crown (Reid and Ferrell, 2005 Mahoney et al., 2016), and formation time is related to human enamel thickness (Dean et al., 2001; Mahoney 2011). Thus, inter-individual variation in the periodicity of the biorhythm may have a clearer association with final enamel thickness through the duration, rather than the daily rate of enamel growth. More work is needed to understand if and how these developmental mechanisms change within a species (**Fig 5**).

The proposal that aspects of enamel growth are controlled by a long-period biological 'clock' with an infradian rhythm, whether it is the HHO via the SCN of the brain, or a

different 'peripheral' independent 'clock' (Hastings, 1998), or even more than one 'clock' (Newman and Poole, 1974, 1993), is a hypothesis. Our data for human permanent teeth, and deciduous teeth (Mahoney et al., 2016, 2017), provide support for this hypothesis. The infradian rhythm (reflected by RP) appears to have an association with final enamel thickness of a crown, but is inconsistently related to the daily *amount* of enamel secreted by ameloblasts as these cells respond to a circadian rhythm (reflected by cross striations). The infradian rhythm likely has a systemic origin, as RP can alter within a single crown in response to non-specific pathology (Mahoney et al., 2017). The longer-period rhythm is intrinsic to enamel growth, not only relating to final enamel thickness, but also the microstructural components of enamel (prisms) which can be reduced in size, or have an altered morphology when associated with Retzius lines (Risnes, 1990,1998; Li and Risnes, 2004). Perhaps therefore, the infradian rhythm periodically modifies ameloblast metabolism, interfering with enamel secretion of ameloblasts, leading to the altered prism structure that can be associated with Retzius lines.

There is substantial residual in the relationship of RP to enamel thickness (Table 1), as even the strongest correlations explain just over half of the variation in our data. So, there are other factors operating as well. Enamel thickness is a product of several mechanisms, other than those considered here, such as the number of active ameloblasts and their life spans (Grine and Martin, 1988; Macho, 1995). We have only considered the rate that enamel grows in thickness, but whether the rate that enamel crowns extend in height (enamel extension rates), as epithelium cells differentiate into pre-ameloblasts down along the dentin-enamel junction (DEJ), is linked to RP, has yet to be determined. Guatelli-Steinberg and colleagues (2012) have already shown links between DEJ lengths and lateral enamel formation time. As RP is correlated with enamel formation times (Reid and Ferrell, 2006; Mahoney et al., 2016), it would seem possible that extension rates can relate to RP.

Retzius line periodicity, femoral length, and osteocyte lacunae density

Our data support the intra-specific HHO prediction that taller adults (with longer femora) have a lower RP (Bromage et al., 2016a). Thus, the biorhythm oscillates with a faster periodicity in taller humans, compared to those with shorter femora. However, we found less support for the prediction that taller adults maintain significantly faster rates of femoral osteocyte proliferation, relative to shorter adults. Osteocyte density did not relate to stature or femoral length amongst our sample of young adult males, though it appeared to be trending towards significance with a high residual amongst older males (Table 2, and footnotes). Neither did RP relate to Ot.Dn in a small sample. Thus, the biorhythm is significantly linked to adult stature, but neither the biorhythm nor stature are linked to osteocyte proliferation of the femur.

Osteocytes have a complex functionality (see Introduction) that, in addition to potential influences of body size, probably influences their distribution in cortical bone leading to significant variation in their numbers across the femoral shaft (e.g., Carter et al. 2013, 2014). For example, an anatomical region can adapt to mechanical loading, adding and removing new bone tissue in response to loading or disuse (Wolff, 1892; Robling et al., 2001; Burr et al., 2002). Our osteocyte lacunae data are from one anatomical region, the posterior femoral mid-shaft cortex, and just the sub-periosteal pocket, which is where new bone is usually deposited in response to excessive load (Robling et al., 2006). There is substantial inter-individual variation in Ot.Dn values from this region (younger adults range between 394.87 and 1307.69; middle aged adults between 305.77 and 1255.13). Some of this variation in Ot.Dn probably reflects differences in femoral mechanical loading between individuals, as some adults in our sample would have been employed in the physically demanding occupations that were typical of lower socio-economic lifestyles in medieval Canterbury (Miszkiewicz and Mahoney, 2016).

Variation in adult stature is not strongly related to differences among individuals in the rate of femoral osteocyte proliferation, but it is related to RP (Table 2). This finding makes sense if RP is linked to the duration in which stature is attained. Pre-pubertal growth velocity differences can underlie adult stature differences within some populations (e.g., Gasser 1990; Gasser et al., 2001), but not all populations. Instead, the timing of the pubertal growth spurt can contribute to the *age* adult height is attained, for females compared to males (e.g., Tanner, 1990; Roche, 1992; Gasser et al., 2000), and within the sexes (Hägg and Taranger, 1991; Baer et al., 2006). Late maturing Swedish boys continued to grow between 18 to 25 years of age, attaining significantly greater growth in height during this period and a greater final stature, compared to early maturing boys whose height increased only slightly after age 18 (Hägg and Taranger, 1991). The Nurses' Health Study (II) in the USA, which is based upon large sample sizes, indicates that females with delayed puberty are older when they attain their final and greater adult height, compared to females with a shorter adult stature (Baer et al., 2006). Further research might explore potential linkages between the frequency that the biorhythm oscillates and the age that adult stature is attained, as the duration of the growth period may be an important link to RP for aspects of both enamel and bone growth. Variation in growth velocities (and Ot.Dn) compared to RP amongst children should also be examined.

The biorhythm of human skeletal growth

The direction of the correlation between RP and enamel thickness is positive, but negative when RP is related to stature. Our data implies that a child from Canterbury with a slow biorhythm between birth and five years of age attained thicker deciduous (Mahoney et al., 2016) and permanent molar enamel, compared to another child with a faster biorhythm that developed thinner enamel (**Fig. 6**). A child from the same population with a fast biorhythm attained a greater adult stature. These findings imply that the biorhythm may coordinate

aspects of human skeletal growth, perhaps by increasing the duration of crown enamel growth early on in ontogeny leading to thicker enamel, at the expense of subsequent femoral growth in length and attained adult height. Alternatively, the change in the direction of the correlation may reflect a biorhythm that does not remain constant within an individual. We have previously shown that RP can change within an individual at the end of the first post-natal year (Mahoney et al., 2017). The change in RP, from deciduous to permanent molars, suggests that the biorhythm produces a sequence of RPs for an individual, rather than a static value. In the present study, we focused on permanent M1s and M2s, whose enamel forms between birth and five to six years of age (Reid and Dean, 2006). It seems likely that RP remains constant during this age-range within an individual, as comparisons between small samples of permanent anterior teeth that form at about the same time as permanent molars (FitzGerald, 1998), as well as comparisons between molar types within four individuals (Reid et al., 1998), reveal no variation in RP. Whether the periodicity of the biorhythm changes in humans beyond 11 years of age, after third molar crown enamel has formed, is unknown. Therefore, the relationship we describe, between RP during the early childhood years and adult stature, might not describe this relationship in later ontogeny, if RP changes closer to adulthood, or, if bone modifies it's response to the biorhythm with age.

Conclusion

We examined the relationship of enamel secretion rates to evidence of a biorhythm retained in human teeth as Retzius line periodicity, and of cortical bone osteocyte proliferation to Retzius periodicity. We found only limited evidence for either of these relationships, but we did find stronger evidence of linkages between RP and permanent molar enamel thickness (end state of enamel growth), and RP and final adult stature (end state of linear growth in long bones). Our findings develop the intra-specific HHO hypothesis suggesting that the biorhythm has a role in human skeletal growth and the development of more than one hard tissue.

Conflict of Interest

The authors have no conflict of interest to declare.

REFERENCES

Antoine D, Hillson S, Dean MC (2009) The developmental clock of dental enamel: a test for the periodicity of prism cross striations and an evaluation of the likely sources of error in histological studies of this kind. *J Anat* **214**, 45–55.

von Asper H (1916) *Uber die Braune Retzius sche Parallelstreifung im Schmelz der menschlichen Zahne*. PhD thesis: Universitat Zurich.

Baer HJ, Rich-Edwards JW, Colditz GA, Hunter DJ, Willett WC, Michels KB (2006) Adult height, age at attained height, and incidence of breast cancer in premenopausal women. *Int J Cancer* **119**, 2231–2235.

Bancroft JD, Gamble M (2008) *Theory and practice of histological techniques*. Elsevier Health Sciences.

Beynon AD (1992) Circaseptan rhythms in enamel development in modern humans and Plio-Pleistocene hominids. In *Structure, Function and Evolution of Teeth* (eds Smith P, Tchernov E), pp. 295-309. London: Freund Publishing House Ltd.

Boas F (1935) The tempo of growth of fraternities. *Proc Nat Acad Sci* **21**, 413-418.

Bonewald LF (2007) Osteocytes as dynamic multifunctional cells. *Ann N Y Acad Sci* **1116**, 281–290.

Boyde A (1979) Carbonate concentration, crystal centres, core dissolution, caries, cross striation, circadian rhythms and compositional contrast in the SEM. *J Dent Res* **58**, 981–983.

Boyde A (1989) Enamel. In: *Teeth. Handbook of microscopic anatomy* (eds Berkovitz BKB, Boyde A, Frank RM, et al.), pp. 309–473. Berlin: Springer-Verlag.

Brent J (1879) *Canterbury in the olden time*. London: Simpkin, Marshall and Co.

Bromage TG (1991) Enamel incremental periodicity in the pigtailed macaque: a polychrome fluorescent labelling study of dental hard tissues. *Am J Phys Anthropol* **86**, 205–214.

Bromage TG, Hogg RT, Lacruz RS. et al. (2012) Primate enamel evinces long period biological timing and regulation of life history. *J Theor Biol* **305**, 131–144.

Bromage TG, Idaghdour Y, Lacruz RS. et al. (2016b) The swine plasma metabolome chronicles 'many days' biological timing and functions linked to growth. *PLoS One* e0145919.

Bromage TG, Juwayeyic YM, Katrisa JA. et al. (2016a) The scaling of human osteocyte lacuna density with body size and metabolism. *C R Palevol* **15**, 32–39.

Bromage TG, Lacruz RS, Hogg R. et al. (2009) Lamellar bone is an incremental tissue reconciling enamel rhythms, body size, and organismal life history. *Calcif Tiss Int* **84**, 388-404.

Buikstra JE, Ubelaker DH (1994) *Standards for data collection from human skeletal remains*. Fayetteville: Arkansas Archaeology Survey.

Burr DB, Robling AG, Turner CH (2002) Effects of biomechanical stress on bones in animals. *Bone* **30**(5), 781–6.

Le Cabec A, Dean MC, Begun DR (2017) Dental development and age at death of the holotype of *Anapithecus hernyaki* (RUD 9) using synchrotron virtual histology. *J Hum Evol* **108**, 161-175.

Carter Y, Suchorab JL, Thomas CD, Clement JG, Cooper DM (2014) Normal variation in cortical osteocyte lacunar parameters in healthy young males. *J Anat* **225**, 328-36.

Carter Y, Thomas CD, Clement JG, Peele AG, Hannah K, Cooper DM (2013) Variation in osteocyte lacunar morphology and density in the human femur--a synchrotron radiation_micro-CT study. *Bone* **52**(1), 126-32.

Cullinane DM (2002) The role of osteocytes in bone regulation: mineral homeostasis versus mechanoreception. *J Musc Neuronal Interact* **2**, 242-4.

Coomans CP, van den Berg SA, Houben T, van Klinken JB, van den Berg R, Pronk AC, Havekes LM, Romijn JA, van Dijk KW, Biermasz NR, Meijer JH (2013) Detrimental effects of constant light exposure and high-fat diet on circadian energy metabolism and insulin sensitivity. *FASEB J* **27**,1721–1732.

Dean MC (1987). Growth layers and incremental markings in hard tissues; a review of the literature and some preliminary observations about enamel structure in *Paranthropus boisei*. *J Hum Evol* **16**, 157–172.

Dean MC (1995) The nature and periodicity of incremental lines in primate dentine and their relationship to periradicular bands in OH 16 (Homo habilis). In *Aspects of Dental Biology: Paleontology, Anthropology and Evolution* (ed Moggi-Cecchi J), pp. 239-265. Florence: International Institute for the Study of Man.

Dean MC, Leakey MG, Reid DJ. et al. (2001) Growth processes in teeth distinguish modern humans from Homo erectus and earlier hominins. *Nature* **414**, 628–631.

Dean MC, Scandrett AE (1996) The relation between long-period incremental markings in dentine and daily cross-striations in enamel in human teeth. *Arch Oral Biol* **41**, 233-241.

Duncombe J (1785) The history and antiquities of the three archiepiscopal hospitals and other charitable foundations at and near Canterbury. *Bibliotheca Topographica Britannica* No XXX, London.

Ferembach D, Schwindezky I, Stoukal M (1980) Recommendations for age and sex diagnoses of skeletons. Journal of Human Evolution 9: 517-549.

FitzGerald CM (1998) Do enamel microstructures have regular time dependency? Conclusions from the literature and a large scale study. *J Hum Evol* **35**, 371-386.

Frost HM (1987) Bone "mass" and the "mechanostat": a proposal. *Anat Rec* **219**, 1-9.

Gasser T (1990) A method for determining the dynamics and intensity of average growth. *An Hum Biol* 17, 459-457.

Gasser T, Sheehy A, Molinari L, Largo RH (2000) Sex dimorphism in growth. *An Hum Biol* **27**, 187-197.

Gasser T, Sheehy A, Molinari L, Largo RH (2001) Growth processes leading to a large or small adult height. *An Hum Biol* **28**, 319-327.

Garde AH, Hansen AM, Skovgaard LT, Christensen JM (2000). Seasonal and biological variation of blood concentrations of total cholesterol, dehydroepiandrosterone sulfate, hemoglobin A(1c), IgA, prolactin, and free testosterone in healthy women. *Clin Chem* **46**(4), 551–559.

Grine FE, Martin LB (1988) Enamel thickness and development in Australopithecus and Paranthropus. In *The evolutionary history of the robust Australopithecines* (ed Grine FE), pp. 3–42. New York: Aldyne de Gruiter.

Guatelli-Steinberg D, Floyd BA, Dean MC, Reid DJ (2012) Enamel extension rate patterns in modern human teeth: two approaches designed to establish an integrated comparative context for fossil primates. *J Hum Evol* **63**, 475–486.

Hägg U, Taranger J (1991) Height and height velocity in early, average and late maturers followed to the age of 25: a prospective longitudinal study of Swedish urban children from birth to adulthood. *Ann Hum Bio* **18(**1**)**, 47-56.

Hasting M (1998) The brain, circadian rhythms, and clock genes. *Brit Med J*, **317**, 1704-1707.

Herman BC, Cardoso L, Majeska RJ, Jepsen KJ, Schaffler MB (2010) Activation of Bone Remodeling after Fatigue: Differential Response to Linear Microcracks and Diffuse Damage. *Bone* **47**(4), 766–772.

Hicks M, Hicks A (2001) *St. Gregory's Priory, Northgate, Canterbury Excavations 1988–1991*. Canterbury Archaeological Trust Ltd: Volume II.

Hogg RT, Godfrey LR, Schwartz GT, Dirks W, Bromage TG (2015) Lemur biorhythms and life history evolution. *PLoS ONE* **10**(8), e0134210. doi:10.1371/journal.pone.0134210

Hunter RL, Agnew AM (2016) Intraskeletal variation in human cortical osteocyte lacunar density: Implications for bone quality assessment. *Bone Reports* **5**, 252-261.

Kalsbeek A, Scheer FA, Perreau-Lenz S. et al. (2011) Circadian disruption and SCN control of energy metabolism. *FEBS Letters* **585**, 1412–1426.

Krogman WM, Iscan MY (1986) The human skeleton in forensic medicine (2nd ed). Springfield: Charles C Thomas. P 156-162

Lacruz RS, Dean MC, Ramirez-Rozzi F, Bromage TG (2008) Megadontia, striae periodicity and patterns of enamel secretion in Plio-Pleistocene fossil hominins. *J Anat.*. **213**, 148–158

Lacruz RS, Bromage TG (2006) Appositional enamel growth in molars of South African fossil hominids. *J Anat* **209**, 13–20.

Lacruz RS, Hacia JG, Bromage TG. et al. (2012) The circadian clock modulates enamel development. *J Biol Rhyth* **27**, 237–245.

Lee CF, Profitt WR (1995) The daily rhythm of tooth eruption. *Am J Orthod Dentofacial Orthop* **107**(1), 38-47.

Li C, Risnes S (2004) SEM observations of Retzius lines and prism cross-striations in human dental enamel after different acid etching regimes. *Arch Oral Biol* **49**, 45-52.

Little MA, Rummel JA (1971) Circadian variations in thermal and metabolic responses to heat exposure. *J Appl Physiol* **31**(4), 556–561.

Lovejoy CO, Meindl RS, Pryzbeck TR, Mensforth TJ (1985) Chronological metamorphosis of the auricular surface of the ilium: A new method for the determination of age at death. *Am J Phys Anthropol* **68**, 15-28.

Macho G (1995) The significance of hominid enamel thickness for phylogenetic and life-history reconstruction. In: Aspects of Dental Biology: Palaeontology, Anthropology and Evolution (ed. Moggi-Cecchi J), pp. 51–68. Florence: International Institute for the Study of Man.

Mahoney P (2008) Intraspecific variation in M1 enamel development 601 in modern humans: implications for human evolution. *J Hum Evo* **55**, 131–147.

Mahoney P (2011) Human deciduous mandibular molar incremental enamel development. *Am J Phys Anthropol,* 144, 204–214.

Mahoney P (2013) Testing functional and morphological interpretations of enamel thickness along the deciduous tooth row in human children. *Am J Phys Anthropol* 151, 518–525.

Mahoney P (2015) Dental fast track: prenatal enamel growth, incisor eruption, and weaning in human infants. *Am J Phys Anthropol* 156, 407–421.

Mahoney P, Miszkiewicz JJ, Pitfield R, Schlecht SH, Deter C, Guatelli-Steinberg D (2016) Biorhythms, deciduous enamel thickness, and primary bone growth in modern human children: a test of the Havers-Halberg Oscillation hypothesis. *J Anat* **228**, 919–928.

Mahoney P, Miszkiewicz JJ, Pitfield R, Deter C, Guatelli-Steinberg D (2017) Enamel biorhythms of humans and great apes: the Havers-Halberg Oscillation hypothesis reconsidered. *J Anat* 230, 272-281.

Mahoney P, Smith TM, Schwartz GT, Dean MC, Kelley J (2007) Molar crown formation in the Late Miocene Asian hominoids, *Sivapithecus parvada* and *Sivapithecus indicus*. *J Human Evol* **53**, 61-68

Martin LB (1983) Relationships of the later Miocene Hominoidea. Ph.D. Dissertation, University College London.

Martin LB (1985) Significance of enamel thickness in hominoid evolution. *Nature* **314**, 260-263.

Meindl RS, Lovejoy CO, Mensforth RP, Walker RA (1985) A revised method of age determination using the os pubis, with a review and tests of accuracy of other current methods of pubic symphyseal aging. *Am J Phys Anth* **68**, 29–45.

Metz LN, Martin RB, Turner AS (2003) Histomorphometric analysis of the effects of osteocyte density on osteonal morphology and remodeling. *Bone* **33**(5), 753-759.

Miszkiewicz JJ (2014) Ancient human bone histology and behaviour. PhD Dissertation. University of Kent: Canterbury, UK.

Miszkiewicz JJ (2016) Investigating histomorphometric relationships at the human femoral midshaft in a biomechanical context. *J Bone Min Metab* **34**(2), 179-192.

Miszkiewicz JJ, Mahoney P (2016) Ancient human bone microstructure in medieval England: comparisons between two socio-economic groups. *Anat Rec* **299**, 42-59.

Mullender MG, Huiskes R, Versleyen H, Buma P (1996) Osteocyte Density and Histomorphometric Parametersin Cancellous Bone of the Proximal Femur in Five Mammalian Species. *J Orth Res* **14**, 972-979.

Mullender MG, Tan SD, Vico L, Alexandre C, Klein-Nulend J (2005). Differences in osteocyte density and bone histomorphometry between men and women and between healthy and osteoporotic subjects. *Calcif Tiss Int* **77**(5), 291-296.

Nakashima T, Hayashi M, Fukunaga T, Kurata K, Oh-Hora M, Feng JQ, Bonewald LF, Kodama T, Wutz A, Wagner EF, Penninger JM, Takayanagi H (2011) Evidence for osteocyte regulation of bone homeostasis through RANKL expression. Nat Med **17**,1231-4.

Newman H, Poole D (1974) Observations with scanning and transmission electron microscopy on the structure of human surface enamel. *Arch Oral Biol* **19**, 1135-1143.

Newman H, Poole D (1993) *Dental enamel growth*. J Roy Soc Med **86**, 61.

Noble BS (2008) The osteocyte lineage. *Arch Biochem Biophys* **473**, 106–111.

Palumbo C, Palazzini S, Marotti G (1990) Morphological study of inter-cellular junctions during osteocyte differentiation. *Bone* **11**, 401–406.

Parfitt AM (1983) Steriologic basis of bone histomorphometry; theory of quantitative microscopy and reconstruction of the third dimension. In: *Bone Histomorphometry: Techniques and Interpretation* (Recker RR, ed). pp, 53–87. Boca Raton, FL: CRC Press.

Phenice TW (1969) A newly developed visual method for sexing the os pubis. *Am J Phys Anthropol* **30**, 297-302.

Ralph MR, Foster RG, Davis FC, Menaker M (1990) Transplanted suprachiasmatic nucleus determines circadian period. *Science* **247**, 975–978.

Reid DJ, Beynon AD, Ramirez Rozzi FV (1998) Histological reconstruction of dental development in four individuals from a medieval site in Picardie, France. J Hum Evol **35**, 463–477.

Reid DJ, Dean MC (2006) Variation in modern human enamel formation times. *J Hum Evol* **50**, 329–346.

Reid DJ, Ferrell R (2006) The relationship between number of striae of Retzius and their periodicity in imbricational enamel formation. *J Hum Evol* **50**, 195–202.

Reinberg A, Sidi E, Ghata J (1965) Circadian reactivity rhythms of human skin to histamine or allergen and the adrenal cycle. *J Allergy* **36**, 273-283.

Retzius A (1837) Bemerkungenq ber den inneren Bau der Zahne, mit besonderer Rücksicht auf dem in Zahnknochen Vorkommenden Röhrenbau. *Arch Anat Physiol* 486–566.
Richter CP (1965) *Biological Clocks in Medicine and Psychiatry*. Springfield, IL: CC Thomas.

Risnes S (1986) Enamel apposition rate and the prism periodicity in human teeth. *Scand J Dent Res* **94**, 394–404.

Risnes S (1990) Structural characteristics of staircase-type retzius lines in human dental enamel analyzed by scanning electron microscopy. *Anatom Rec* **226**, 135–146.

Risnes S (1998) Growth tracks in dental enamel. *J Hum Evol* **35**, 331-350.

Robling AG, Duijvelaar KM, Geevers JV, Ohashi N, Turner CH (2001) Modulation of appositional and longitudinal bone growth in the rat ulna by applied static and dynamic force. *Bone,* **29**, 105–113.

Robling AG, Castillo AB, Turner CH (2006) Biomechanical and molecular regulation of bone remodeling. *Annu Rev Biomed Eng* **8**, 455-498.

Robling AG, Turner CH (2002). Mechanotransduction in bone: genetic effects on mechanosensitivity in mice. *Bone* **31**(5), 562-569.

Roche AF (1992) Growth, maturation and body composition. The Fels longitudinal study 1929-1991. Cambridge University Press.

Schour I, Poncher HG (1937) Rate of apposition of enamel and dentin, measured by the effect of acute fluorosis. *Am J Dis Child* **54**, 757–776.

Schwartz GT, Mahoney P, Godfrey LR, Cuozzo FP, Jungers WL, Randria GFN (2005) Dental development in *Megaladapis edwardsi* (primates, lemuriformes): implications for understanding life history variation in subfossil lemurs. *J Hum Evol* **49**, 702-721.

Schwartz GT, Reid DJ, Dean C (2001) Developmental aspects of sexual dimorphism in hominoid canines. *Int J Primatol* **22**, 837–860.

Schwartz GT, Samonds KE, Godfrey LR, Jungers WL, Simons EL (2002) Dental microstructure and life history in subfossil Malagasy lemurs. *Proc Natl Acad Sci USA* **99**, 6124-6129.

Schwartz JH (1995) Skeleton Keys. Oxford University Press.

Smith TM (2008) Incremental dental development: methods and applications in hominoid evolutionary studies. *J Hum Evol,* **54**, 205–224.

Smith TM, Dean MC, Kelley J, Martin LB, Reid DJ, Schwartz GT (2003) Molar crown formation in Miocene hominoids: a preliminary synthesis. *Am J Phys Anthropol.* **36** (Suppl.), 196.

Somner W (1703) *The antiquities of Canterbury*. EP Publishing Limited.

Sothern RB (1974) Chronobiologic serial section on 8876 oral temperatures collected during 4.5 years by presumably healthy man (age 20.5 at start of study). In *Chronobiology* (eds Scheving LE, Halberg F, Pauly JE), pp. 245–248. Tokyo: Igaku Shoin Ltd.

Sujino M, Masumoto K, Yamaguchi S, van der Horst GT, Okamura H, Inouye SI (2003) Suprachiasmatic nucleus grafts restore circadian behavioral rhythms of genetically arrhythmic mice. *Curr Biol* **13**(8), 664–668.

Tanner JM (1990) Fetus into man: physical growth from conception to maturity. Cambridge, MA: Harvard University Press.

Tatsumi S, Ishii K, Amizuka N, Li M, Kobayashi T, Kohno K, Ito M, Takeshita S, Ikeda K (2007) Targeted ablation of osteocytes induces osteoporosis with defective mechanotransduction. *Cell Metab* **5**, 464-75.

Teti A, Zallone A (2009) Do osteocytes contribute to bone mineral homeostasis? Osteocytic osteolysis revisited. *Bone* **44**, 11–16.

Trotter M (1970) Estimation of stature from intact long bones. In *Personal Identification in Mass Disasters* (eds Stewart TD), pp. 71–83. Washington, DC: Smithsonian Institution Press.

Verborgt O, Gibson GJ, Schaffler MB (2000) Loss of osteocyte integrity in association with microdamage and bone remodeling after fatigue in vivo. *J Bone Miner Res* **15**, 60–7.

van Hove RP, Nolte PA, Vatsa A, Semeins CM, Salmon PL, Smit TH, Klein-Nulend J (2009) Osteocyte morphology in human tibiae of different bone pathologies with different bone mineral density—is there a role for mechanosensing? *Bone* **45**(2), 321-329.

Weaver D (1998) The Suprachiasmatic Nucleus: A 25-Year Retrospective. *J Biol Rhythms* **13**(2): 100-112.

White T D, Black MT, Folkens PA (2011) *Human Osteology*. 3rd ed. Boston: Academic Press.

Wolff J (1982) Das Gesetz der Transformation der Knochen. Berlin: Hirschwald.

Zheng L, Seon YJ, Mourão MA. et al. (2013). Circadian rhythms regulate amelogenesis. *Bone* **55**, 158–165.

Table 1 Linear regression analyses of log-Retzius periodicity against log-enamel growth.

ENAMEL	*n*	Intercept	Slope	*r*	r^2	*p*	Residual
Thickness. RP v EA							
All	40	0.755	0.569	0.697	0.486	<0.001*	55%
M1	25	0.826	0.489	0.615	0.378	0.001*	64%
M2	15	0.639	0.703	0.806	0.650	<0.001*	43%
Thickness. RP v AET							
All	40	-0.426	0.432	0.604	0.365	0.002*	63%
M1	25	-0.391	0.384	0.577	0.333	0.004*	68%
M2	15	-0.542	0.580	0.720	0.519	0.002*	44%
Rate. RP v DSR							
M1	15	0.817	-0.098	0.009	0.000	0.714	98%

Tooth types: M1, permanent first molar; M2, permanent second molar. *Significant. EA: Enamel area. AET: Average enamel thickness. DSR: Daily secretion rate. RP: Retzius periodicity. **RP v EA**: Lower M1 (n=13): r^2= 0.491, p= 0.007*. Upper M1 (n=12): r^2= 0.633, p= 0.001*. Lower M2 (n=12): r^2= 0.603, p= 0.002*. **RP v AET**: Lower M1 (n=13): r^2= 0.338, p= 0.037*. Upper M1 (n=12): r^2= 0.482, p= 0.012*. Lower M2 (n=12): r^2= 0.287, p= 0.072. Upper M2 excluded from separate analysis as n=3.

Table 2 Linear regression analyses of log-Retzius periodicity against log-bone growth.

BONE	*n*	Intercept	Slope	*r*	r^2	*p*	Residual
Stature. RP v S[a]							
Younger M	27	2.309	-0.082	-0.417	0.213	0.015*	74%
Rate. RP v Ot.Dn							
Younger M	10	3.232	-0.401	-0.370	0.159	0.326	90%
Rate. S v Ot.Dn[b]							
Younger M	28	2.171	0.019	0.199	0.039	0.317	94%
Older M	94	2.185	0.016	0.175	0.030	0.089	93%

S: Estimated stature. RP: Retzius periodicity. M: Males. Ot.Dn: Osteocyte lacunae density.

[a]Femoral length v RP: Young M intercept= 3.232, slope= -0.135, r=-0.492, p=0.020*.

[b]Ot.Dn v femoral length: Young M intercept= 1.567, slope= 0.030, r=0.199, p=0.317. Older M intercept= 1.587, slope= 0.025, r=0.176, p=0.088.

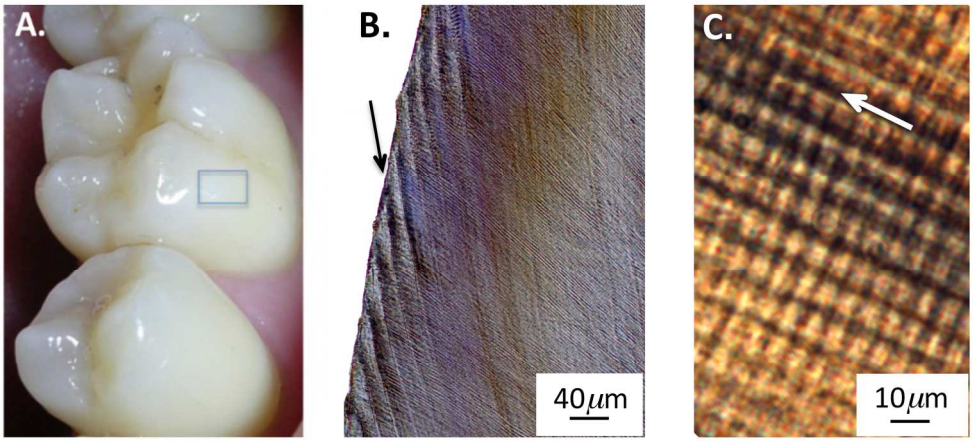

Fig 1. Human first molar with lateral enamel highlighted (A), black arrow points to infradian Retzius line (B), white arrow points in direction of prisms, with circadian cross striations at right angle to the arrow (C).

179x83mm (300 x 300 DPI)

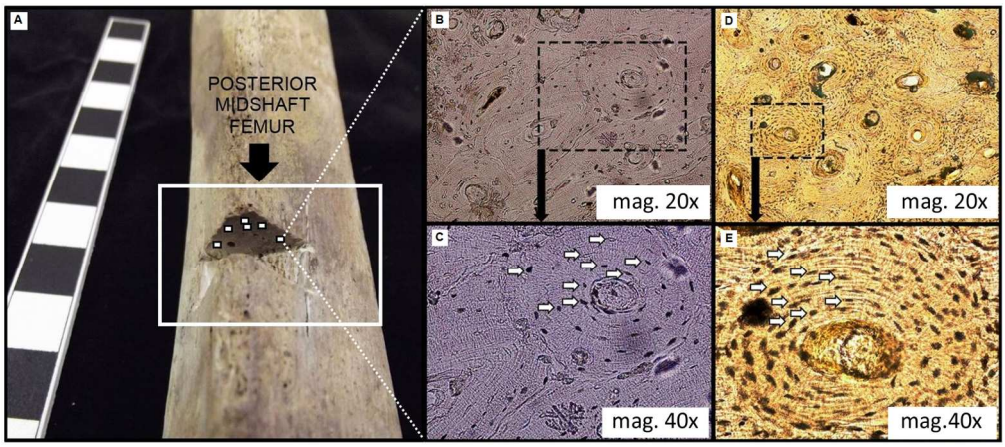

Fig 2. The figure illustrates the regions of interest (ROI) in the posterior mid-shaft femur (A). The sectioned cortical location is highlighted, with approximate (not to scale) positioning of ROIs adjacent to the periosteum (these are placed on the superior region in the sectioned area only for illustrative purposes in this figure, as we examined the removed cortical bone). The series of four histology images on the right show lower (B, and magnified in C) and higher densities (D, and magnified in E) of osteocyte lacunae (white arrows).

149x65mm (300 x 300 DPI)

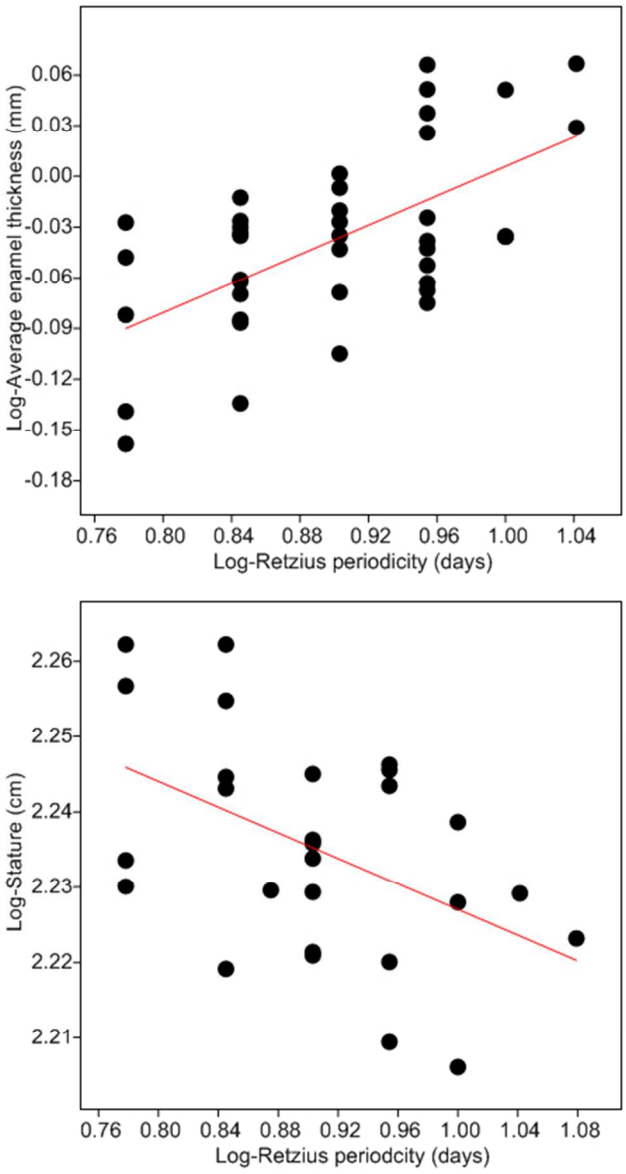

Fig. 3 Plot of log-Retzius line periodicity against log-average enamel thickness for all molar types combined n=40 (A) and the stature of young males n=27 (B). Regression lines are fitted to the data. Regression statistics are in Table 1. Corresponding data sets are available in Supporting Information.

39x72mm (300 x 300 DPI)

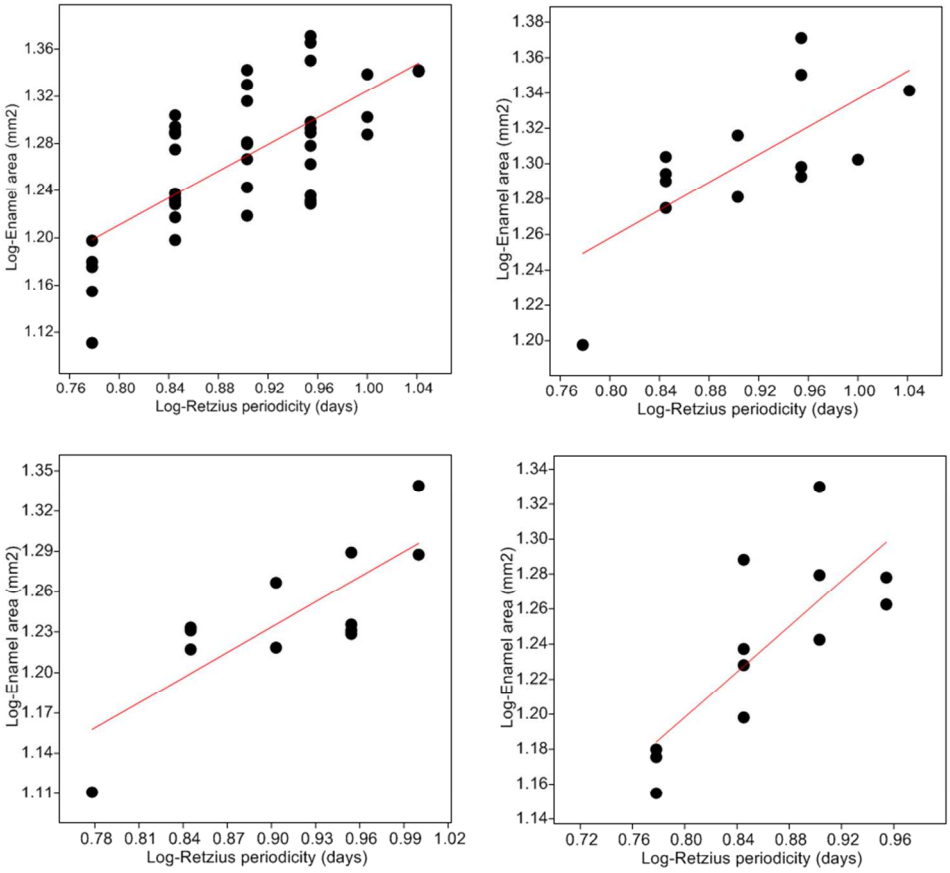

Fig. 4 Plot of log-Retzius periodicity against log-enamel area with regression lines fitted to the data. All molar types combined n=40 (A), which are separated into tooth types for lower first molars (B), upper first molars (C), and lower second molars (D). Upper second molars (n=3) are excluded from separate analysis because of the small sample size. Regression statistics are in Table 1 and footnotes. Corresponding data sets are available in Supporting Information.

83x75mm (300 x 300 DPI)

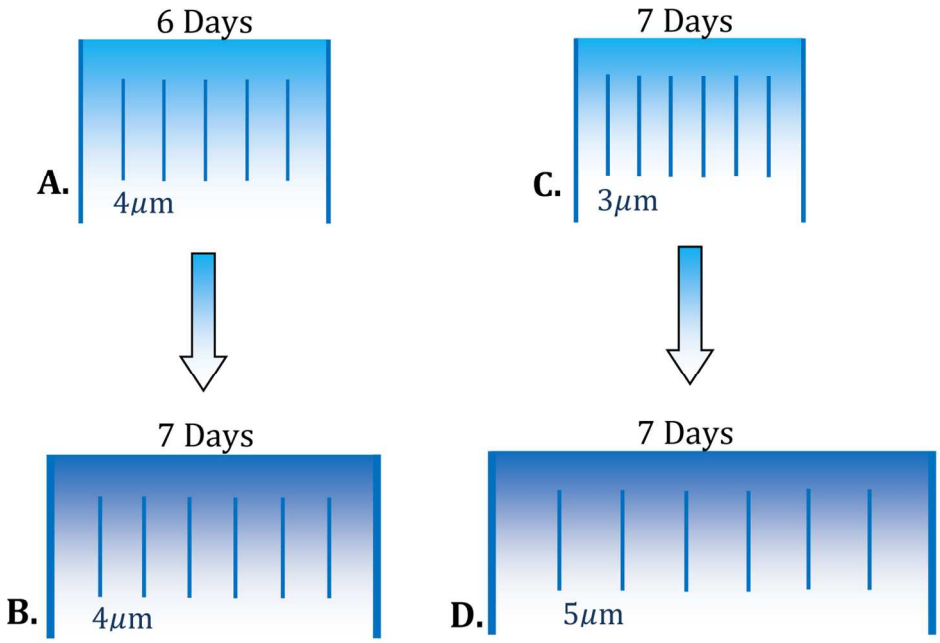

Fig 5. Cell mechanisms underlying different thicknesses of human enamel layers. Long lines illustrate two adjacent Retzius lines (enamel layer) in one outer lateral region of the crown. Short lines represent daily cross striations with either 3, 4 or 5μm of enamel between adjacent striations, representing different daily enamel secretion rates (DSR). Retzius periodicity increases from six days in A to seven days in B. Layer B increases in width because ameloblasts have secreted enamel for an extra day, relative to A, but the DSR remains constant (e.g., this study, and Mahoney et al., 2017). Another developmental mechanism is illustrated by C and D. Retzius periodicity remains the same in both illustrations. Layer D increases in width because of the greater DSR, relative to C, which might be expected when deciduous incisors are compared to second molars along the tooth row of the same individual (Mahoney, 2015).

134x93mm (300 x 300 DPI)

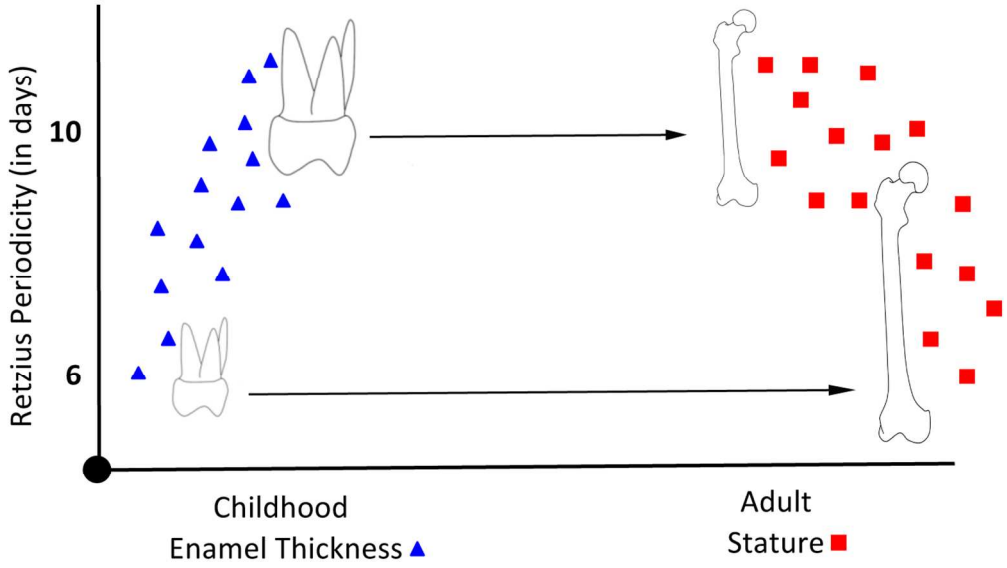

Fig 6. Hypothetical relationship between Retzius line periodicity, and the final enamel thickness of a tooth crown, and final attained adult stature.

118x70mm (300 x 300 DPI)

SUPPORTING INFORMATION

The Biorhythm of Human Skeletal Growth

Patrick Mahoney[1], Justyna J. Miszkiewicz[2], Simon Chapple[1], Mona Le Luyer[3], Stephen H. Schlecht[4], Tahlia J. Stewart[2], Richard A. Griffiths[5], Chris Deter[1], Debbie Guatelli-Steinberg[6]

[1]Human Osteology Lab, Skeletal Biology Research Centre, School of Anthropology and Conservation, University of Kent, Canterbury, UK.
[2]School of Archaeology and Anthropology, Australian National University, Canberra, Australia.
[3]De la Prehistoire a l'Actuel Culture Environment et Anthropologie (PACEA), University of Bordeaux, Aquitaine, France.
[4]Department of Orthopaedic Surgery, University of Michigan, Ann Arbor, MI, USA.
[5]Durrell Institute of Conservation and Ecology, School of Anthropology and Conservation, University of Kent.
[6]Department of Anthropology, The Ohio State University, Columbus, OH, USA .

Table S1 Retzius periodicity (RP), enamel area, and average enamel thickness measurements for juveniles. Abbreviations: Low M1, lower first molar; Low M2, lower second molar; Up M1, upper first molar; Up M2, upper second molar. One tooth represents one individual.

Project n	Tooth type	Age category	RP (days)	Enamel area (mm^2)	AET (mm)
1	Low-M1	Juvenile	6	15.76	0.82773109
2	Low-M1	Juvenile	11	21.95	1.06864654
3	Low-M1	Juvenile	9	23.5	1.12601821
4	Low-M1	Juvenile	9	19.62	0.91596639
5	Low-M1	Juvenile	7	18.83	0.92576205
6	Low-M1	Juvenile	8	19.1	0.93996063
7	Low-M1	Juvenile	10	20.06	0.92145154
8	Low-M1	Juvenile	7	19.5	0.85152838
9	Low-M1	Juvenile	8	20.7	0.9059081
10	Low-M1	Juvenile	9	22.41	1.06107955
11	Low-M1	Juvenile	7	20.13	0.94109397
12	Low-M1	Juvenile	9	19.87	0.88626227
13	Low-M1	Juvenile	7	19.69	0.97138629
14	Low-M2	Juvenile	8	21.38	1.00328484
15	Low-M2	Juvenile	6	15.13	0.89579633
16	Low-M2	Juvenile	9	18.97	1.09022989
17	Low-M2	Juvenile	7	17.27	0.92254274
18	Low-M2	Juvenile	7	15.78	0.82230328
19	Low-M2	Juvenile	7	19.42	0.73436254
20	Low-M2	Juvenile	8	17.48	0.85351563
21	Low-M2	Juvenile	7	16.91	0.93322296
22	Low-M2	Juvenile	9	18.3	0.94524793
23	Low-M2	Juvenile	8	19.03	0.9228904
24	Low-M2	Juvenile	6	14.98	0.93918495
25	Low-M2	Juvenile	6	14.28	0.72634791
26	Up-M1	Juvenile	6	12.91	0.69428925
27	Up-M1	Juvenile	10	19.39	0.92157795
28	Up-M1	Juvenile	9	16.93	0.85591507
29	Up-M1	Juvenile	7	16.49	0.81917536
30	Up-M1	Juvenile	8	16.54	0.78537512
31	Up-M1	Juvenile	10	21.82	1.12532233
32	Up-M1	Juvenile	9	17.2	0.90669478
33	Up-M1	Juvenile	7	17.03	0.86887755
34	Up-M1	Juvenile	9	19.46	0.8413316
35	Up-M1	Juvenile	8	18.48	0.95454545
36	Up-M1	Juvenile	9	17.03	0.86490604
37	Up-M1	Juvenile	7	17.11	0.86632911
38	Up-M2	Juvenile	8	22	0.98434004
39	Up-M2	Juvenile	9	23.2	1.16407426
40	Up-M2	Juvenile	11	21.99	1.16592386

Table S2 Osteocyte density, and estimated stature (from femoral length) for younger and older adult males.

Project n	Sex	Age Category *(y: 18-34yrs, m: 35-50yrs)*	Side	Ot.Dn	Estimated Stature (cm)
41	M	Younger adult	left	607.69	177.08
42	M	Younger adult	right	394.87	163.99
43	M	Younger adult	right	415.38	170.89
44	M	Younger adult	right	426.92	167.56
45	M	Younger adult	right	532.05	161.61
46	M	Younger adult	right	540.38	178.98
47	M	Younger adult	right	543.59	163.51
48	M	Younger adult	right	590.38	167.32
49	M	Younger adult	right	640.00	169.94
50	M	Younger adult	right	656.41	168.75
51	M	Younger adult	right	660.00	166.13
52	M	Younger adult	right	671.16	168.75
53	M	Younger adult	left	684.62	172.32
54	M	Younger adult	right	715.38	169.70
55	M	Younger adult	left	761.54	161.61
56	M	Younger adult	right	769.23	160.89
57	M	Younger adult	right	776.92	166.13
58	M	Younger adult	right	792.31	168.99
59	M	Younger adult	right	820.51	162.56
60	M	Younger adult	right	844.62	165.89
61	M	Younger adult	right	858.97	170.89
62	M	Younger adult	right	897.44	166.84
63	M	Younger adult	right	1055.39	166.37
64	M	Younger adult	right	1062.82	166.61
65	M	Younger adult	left	1098.72	173.03
66	M	Younger adult	right	1144.23	179.22
67	M	Younger adult	right	1307.69	175.17
68	M	middle-aged	right	346.15	177.79
69	M	middle-aged	right	392.31	165.65
70	M	middle-aged	right	465.65	164.70
71	M	middle-aged	right	474.36	172.08
72	M	middle-aged	right	480.77	172.79
73	M	middle-aged	right	692.31	169.94
74	M	middle-aged	right	1255.13	170.18
75	M	middle-aged	right	305.77	169.46
76	M	middle-aged	right	365.38	179.46
77	M	middle-aged	right	376.92	178.27
78	M	middle-aged	right	383.08	169.94
79	M	middle-aged	right	403.85	176.36
80	M	middle-aged	right	421.16	171.84

Table S2 Osteocyte density, and estimated stature for younger and older adult males.

Project n	Sex	Age Category *(y: 18-34yrs, m:35-50yrs)*	Side	Ot.Dn	Estimated Stature (cm)
81	M	middle-aged	right	441.03	177.08
82	M	middle-aged	right	442.31	167.56
83	M	middle-aged	right	461.54	165.42
84	M	middle-aged	right	480.77	169.94
85	M	middle-aged	right	483.33	165.89
86	M	middle-aged	right	494.23	160.42
87	M	middle-aged	right	503.85	168.03
88	M	middle-aged	right	511.54	162.08
89	M	middle-aged	right	512.82	168.03
90	M	middle-aged	right	516.67	173.27
91	M	middle-aged	right	517.31	164.70
92	M	middle-aged	right	520.00	174.94
93	M	middle-aged	right	525.64	170.89
94	M	middle-aged	right	534.62	166.37
95	M	middle-aged	right	538.46	168.27
96	M	middle-aged	right	538.47	165.42
97	M	middle-aged	right	546.16	166.84
98	M	middle-aged	right	548.08	173.27
99	M	middle-aged	right	551.28	166.13
100	M	middle-aged	right	557.69	163.75
101	M	middle-aged	right	563.08	168.51
102	M	middle-aged	right	563.46	170.89
103	M	middle-aged	right	565.38	163.75
104	M	middle-aged	right	569.23	161.13
105	M	middle-aged	right	578.46	166.84
106	M	middle-aged	left	578.21	164.94
107	M	middle-aged	right	579.49	172.32
108	M	middle-aged	right	582.05	166.13
109	M	middle-aged	right	597.44	161.37
110	M	middle-aged	right	601.92	167.56
111	M	middle-aged	right	611.54	162.80
112	M	middle-aged	left	615.38	169.70
113	M	middle-aged	right	624.17	166.13
114	M	middle-aged	right	634.62	176.36
115	M	middle-aged	right	635.90	172.79
116	M	middle-aged	right	638.46	165.65
117	M	middle-aged	left	650.00	173.51
118	M	middle-aged	right	651.28	169.94

Table S2 Osteocyte density, and estimated stature for younger and older adult males.

Project n	Sex	Age Category *(y:18-34yrs, m:35-50yrs)*	SIDE	Ot.Dn	Estimated Stature (cm)
119	M	middle-aged	right	659.62	178.98
120	M	middle-aged	left	667.31	167.56
121	M	middle-aged	right	669.23	178.27
122	M	middle-aged	right	669.23	163.51
123	M	middle-aged	right	687.18	172.32
124	M	middle-aged	right	689.75	167.56
125	M	middle-aged	right	692.31	169.94
126	M	middle-aged	right	711.54	168.51
127	M	middle-aged	right	714.10	165.89
128	M	middle-aged	right	715.38	167.56
129	M	middle-aged	right	730.77	168.51
130	M	middle-aged	right	730.77	170.89
131	M	middle-aged	right	746.15	168.75
132	M	middle-aged	right	776.92	167.56
133	M	middle-aged	right	782.05	167.08
134	M	middle-aged	right	792.31	177.08
135	M	middle-aged	right	794.87	167.56
136	M	middle-aged	right	798.46	177.08
137	M	middle-aged	left	805.77	175.65
138	M	middle-aged	left	812.82	181.12
139	M	middle-aged	right	813.46	161.61
140	M	middle-aged	right	817.95	178.27
141	M	middle-aged	right	834.62	165.42
142	M	middle-aged	left	841.02	174.94
143	M	middle-aged	right	841.54	169.94
144	M	middle-aged	right	844.62	169.22
145	M	middle-aged	left	846.15	170.89
146	M	middle-aged	right	851.28	170.65
147	M	middle-aged	right	867.69	175.17
148	M	middle-aged	right	869.23	170.89
149	M	middle-aged	right	917.95	167.32
150	M	middle-aged	right	923.08	170.41
151	M	middle-aged	right	924.36	175.65
152	M	middle-aged	left	925.64	173.51
153	M	middle-aged	left	998.08	175.41
154	M	middle-aged	right	1000.00	174.70
155	M	middle-aged	left	1000.00	172.32
156	M	middle-aged	left	1030.77	175.65

Table S2 Osteocyte density, and estimated stature for younger and older adult males.

Project n	Sex	Age Category *(y: 18-34yrs, m: 35-50yrs)*	Side	Ot.Dn	Estimated Stature (cm)
157	M	middle-aged	right	1051.28	174.46
158	M	middle-aged	right	1165.38	168.51
159	M	middle-aged	right	1205.13	178.03
160	M	middle-aged	right	1230.77	167.80
161	M	middle-aged	right	1230.77	176.84

Table S3 Retzius periodicity (RP), and estimated stature in young adult males. Abbreviations: Low M1, lower first molar; Low M2, lower second molar; Up M1, upper first molar; Up M2, upper second molar.

Project n	Tooth type	Age Category *(y: 18-34yrs)*	RP	Estimated stature (cm)
272	Up-M1	Younger adult male	7	175.03
273	Low-M2	Younger adult male	8	172.32
274	Low-M2	Younger adult male	7	165.65
275	Low-M1	Younger adult male	9	176.02
276	Low-M2	Younger adult male	9	176.3
277	Low-M2	Younger adult male	8	166.33
278	Low-M2	Younger adult male	8	166.5
279	Low-M2	Younger adult male	7	179.81
280	Low-M2	Younger adult male	6	169.87
281	Low-M2	Younger adult male	9	161.97
282	Low-M2	Younger adult male	10	160.74
283	Low-M2	Younger adult male	6	182.91
284	Up-M1	Younger adult male	7	175.64
285	Up-M1	Younger adult male	8	172.14
286	Low-M1	Younger adult male	8	169.57
287	Low-M2	Younger adult male	6	180.62
288	LowM2	Younger adult male	10	173.25
289	Low-M1	Younger adult male	12	167.19
290	Low-M2	Younger adult male	8	171.35
291	Up-M1	Younger adult male	10	169.04
292	Low-M1	Younger adult male	8	175.8
293	Up-M1	Younger adult male	11	169.5
294	Low-M2	Younger adult male	6	171.25
295	Low-M1	Younger adult male	9	175.17
296	Up-M2	Younger adult male	9	166.00
297	Up-M2	Younger adult male	7	169.66
298	Low-M2	Younger adult male	7	182.91

58